BMC Neuroscience

RESEARCH

Open Access

Platelet-rich fibrin and silver nano-particles loaded chitosan treatment for post-laminectomy epidural scar adhesions: in vivo rats study model

Samah Fouad[1], Awad Rizk[2*], Esam Mosbah[2], Mostafa M. Nabeeh[3], Walaa Awadin[4], Ayman S. Elmezayyen[5,6], Ekramy Elmorsy[7*] and Adel Zaghloul[2]

Abstract

Objective Epidural scar fibrosis commonly leads to functional disability and pain following spinal surgery and is a prevalent manifestation of Failed Back Surgery Syndrome (FBSS). This study aimed to evaluate the use of silver nano-articles (AgNPs) loaded on chitosan (Chi/Ag-NPs) with platelets-rich fibrin (PRF) gel for the reduction of post-laminectomy epidural scar adhesions.

Methods A total of 90 male Sprague Dawley rats (255 ± 55gm) were randomized in-to six groups, each group with 15 rats: control group, laminectomy group, PRF group, Chi/Ag-NPs group, combined treatment group (PRF + Chi/Ag-NPs), and a group to prepare PRF. Lumbar laminectomy procedures were performed between L3-L5 in all rats except the control group. After a 30-days follow-up, macroscopic examination, histological studies, and mRNA evaluation for TGFβ-1and IL-6, were conducted.

Results Data revealed that epidural scar adhesion, scaring, arachnoid involvement, dural thickness, as well as inflammation and TGFβ-1and IL-6 coding genes expression were significantly reduced in PRF group, Chi/Ag-NPs group, and combined group compared to the laminectomy group. Combined treatment showed more significant better outcomes.

Conclusion The use of PRF with Chi/Ag-NPs as nano biomaterials could be considered a combination therapy for the reduction of EF post-laminectomy in a rat model.

Keywords Epidural scar fibrosis, Laminectomy, Platelets-rich fibrin, Silver nanoparticle loaded chitosan

*Correspondence:
Awad Rizk
awadrizk2010@mans.edu.eg
Ekramy Elmorsy
Ekramy.elmorsy@nbu.edu.sa
Full list of author information is available at the end of the article

Introduction

Lumbar laminectomy is widely regarded as the most commonly recognized treatment for lumbosacral disorders [1]. Patients with Failed back surgery syndrome (FBSS) or post-laminectomy syndrome experience persistent pain in the lower back and /or legs [2, 3]. To date, determining the primary cause of postoperative back pain after lumbar spine surgeries remains challenging. The most prevalent causes include foreign body reaction, spinal stenosis, pseudoarthrosis, recurrent disc herniation, root degeneration, spinal instability, and operations on Epidural scar fibrosis and inaccurate spinal level [4].

Epidural scar fibrosis refers to the formation of scar tissue or fibrosis in the surgical area of the spine. This scar tissue surrounds and sticks to the epidural and /or lateral nerve roots, leading to pain following spine surgery as well as functional disability [5]. Multiple clinical and experimental studies have been conducted on substances aimed at preventing or reducing EF after laminectomy [6–11]. Additionally, Metformin [12], berberine [13], Tubastatin A [14], Laminin α1 [15], Tranexamic acid [6], and medical ozone treatment [16] were evaluated.

Platelets-rich fibrin (PRF), Chitosan (Chi), as well as Silver nanoparticles (AgNPs) were shown have beneficial effect for wound healing with proper tissue regeneration and decreased sacring for different mechanisms. PRF is a platelet and immune concentrate, it contains all the components of a blood sample that are beneficial for promoting immunity, healing. PRF can also reduce the density of chronic inflammation cells after laminectomy in rats, enhances tissue healing, angiogenesis, and osteoblast proliferation through cytokines and growth factors released from platelets [17]. Chitosan (Chi) has been extensively utilized in transdermal drug delivery as well as tissue engineering [18]. Chi utilization with triple compression bandage have been found to enhance venous leg ulcers [19]. The Chi barrier demonstrates efficacy in alleviating peridural adhesions in a post-laminectomy rabbit model [20]. While, Silver nanoparticles (AgNPs) had shown broad-spectrum antibacterial activity have been developed [21]. AgNPs have been utilized as adjunctive agent, following burn injuries, and resulting in diminished inflammation as well as faster wound healing [22], suppressing cytokine production and fibroblast proliferation [23, 24]. AgNPs have been used in fields such as drug delivery [25], bone tissue engineering [26], and wound-healing [27].

There are no prior studies about the use of Chi/Ag-NPs for the reduction of EF post-laminectomy, either in human beings or in experimental animals. Consequently, this study aimed to evaluate the efficacy of Chi/Ag-NPs with or without PRF for the reduction of lumber EF in a laminectomy rat model via macroscopical, histopathological, and mRNA expressional levels of IL-6 and TGFβ-1.

Materials and methods

Preparation of (Chi-AgNPs)

Materials

Chi (medium molecular weight, with deacetylation of 85%) was purchased from Acros Organic—New Jersey (USA). The electrochemical cell consists of a platinum (Pt) and silver (Ag) sheet (99.9% purity, Sigma Aldrich-St. Louis, USA). The reagents were used as received.

Preparation of (Chi-AgNPs) solution

The electrochemical method was used to prepare AgNPs within a chitosan matrix (CS-AgNPs) in situ. Briefly, 1%(w/v) of Chi powder was dissolved using 1 M of aqueous citric acid, with a concentration of 7% (v/v). Under applied potential 1.5 v using a power supply, ECOS on a cell consists of a platinum sheet (as cathode) and a silver sheet (as anode) separated by 1 cm immersed in the Chi solution under constant stirring at 450 rpm at the ambient condition. The process was carried out for two hours. AgNPs formation was detected due to the solution's color changing from transparent to yellow [28].

Characterization of Chi/Ag-NPs

Chi/Ag-NPs characterization was conducted via UV–visible spectroscopy, Zeta potential, TEM, as well as ICP studies. UV–visible spectroscopy via Double Beam spectrophotometer (T80 double beam UV–vis spectrophotometer, pg instruments, UK) was used to investigate the in situ electrochemical synthesis of Ag-NPs within the electrolyte of a Chi solution at a wavelength of 250 nm. The zeta potential of AgNPs within the polymer matrix CS was measured utilizing the Zeta size Nano-zs90 instrument (Malvern instruments, Malvern, UK). TEM was conducted to study the formation of spherical AgNPs within the Chi matrix by TEM (JEOL TEM-2100). Finally, ICP analysis was performed in order to quantify the concentration of silver (Ag) using inductively coupled plasma spectrometry (ICP–MS, Agilent 7700X, Australia).

Animals

This study utilized a cohort of 90 adult male Sprague Dawley rats (255 ± 55 g), obtained from the medical experimental research center (MERC), Mansoura University. The study design was approved the Local Ethical Committee, Faculty of Veterinary medicine, Mansoura University (registration number; Ph.D./102). Ethical guidelines of the Ethics committee of national research Center-Egypt for research animal handling were applied.

Study design

The rats were divided randomly into five groups (15 per group), which were classified as the follows (Fig. 1): group A. Control Group (N = 15); group B. Laminectomy group without treatment (N = 60): laminectomy was performed and rats received no treatment, group C PRF treated group (N = 15):: Laminectomy was performed and PRF was applied after laminectomy on dura mater, group D. Chi/Ag-NPs treated group (N = 15): Chi/Ag-NPs were applied post- laminectomy on the dura mater, and group E. Combined PRF with Chi/Ag-NPs (N = 15): Both Chi/Ag-NPs and PRF were applied separately (without mixing) post- laminectomy on the dura mater. Group F. PRF preparation group (N = 15). Blood samples were obtained from donor animals to prepare PRF.

Preparation of the PRF

According to Dohan et al. [29] blood samples were collected from 15 donor animals prior the surgical procedures via cardiac puncture. Briefly, 5 ml of blood was extracted into a glass centrifuge tube and centrifuged for 10 min at speed of 3,000 rpm (RCF = 402 × g) at a 45^0-rotor angulation with a radius of 40 mm, resulting in three centrifugation strata were obtained: a fibrin clot (PRF), located in the middle of the tube, was collected. A durable self-derived fibrin membrane was subsequently obtained by expelling the serum from the clot.

Laminectomy surgical procedure

Rats were generally anesthetized utilizing intraperitoneal injection (a mixture of 10 mg/kg Xylazine Hcl and 75 mg/kg ketamine Hcl). The rats were positioned in a prone position. Following the sterile preparation of their lower backs, a longitudinal incision was performed in the skin along the midline between the dorsal spinous processes of the L3 and L5. The lumbosacral fascia was opened longitudinally, followed by dissection of paraspinal muscles on both sides in a subperiosteal manner to expose the laminae in L3–L5 region. A complete laminectomy was conducted at the L3 vertebra level, followed by the excision of the ligamentum flavum and epidural adipose tissue from the surgical area. The dura mater was fully exposed and left intact. Cotton pads were used to achieve hemostasis. The rats were sacrificed after 30 days using over dosage (120 mg/ kg) of thiopental sodium intraperitoneally. Rats were euthanized in a humane manner. Subsequently, intracardial perfusion was carried out using a 4% paraformaldehyde solution. Five rats were randomly chosen, and their surgical sites were reopened carefully for macroscopic examination, while the other ten rats were used for histopathological evaluation.

Macroscopic grading of epidural scar adhesion

Epidural scar fibrosis degree (at the L3–L5 level) was determined in randomly selected 5 rats based on the Rydell classification [30] (grade 0 = epidural scar tissue indicates non- adherence to the dura mater; grade 1 = indicates epidural scar tissue adherence to the dura mater but could be easily dissected; grade 2 = indicates epidural scar tissue adherence to the dura mater and challenging to separate without damaging the dura mater; and grade 3 = denotes epidural scar tissue was firmly adherent to the dura mater and could not be dissected). Two independent experts, unaware of the experimental groups, conducted macroscopic evaluations of the rats' lesions. Each expert submitted an independent evaluation, and inter-rater reliability was computed. In

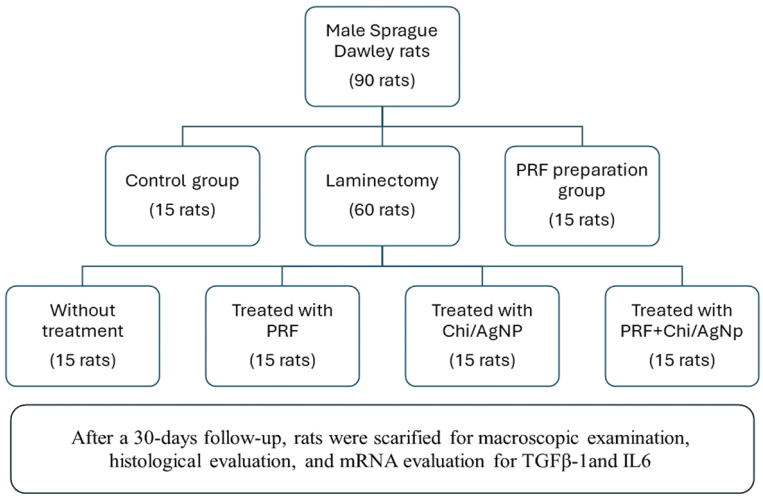

Fig. 1 Schematic diagram for the rats grouping in the study design

instances of discord, a consensus was attained following collaborative examination.

Histopathological evaluation

For histopathological examination, ten rats were selected from each group. En-bloc vertebral columns between L3 and L5 were removed after sacrifice and placed into the 10% Neutral-buffered formaldehyde solution for five days. The specimens were subsequently decalcified in 10% EDTA (Sigma Aldrich, St Louis, MO, USA) for three weeks according to Sangeetha et al. [31] and then embedded in paraffin. Three consecutive sections were obtained from region's distal, middle and proximal parts and then placed in sampling cassettes. Additionally, 5 µm axial sections of the laminectomy site were stained with (H&E) [32] and Masson stain [33]. Then epidural scar adhesions were assessed utilizing a light microscope.

Quantitative morphometric analysis

Masson-stained sections were subjected to quantitative morphometric analysis using image analysis software (Image J, 1.46a, NIH, USA). Two independent pathologists, unaware of the experimental groups, conducted histopathological evaluations of the tissue slides. Each pathologist submitted their evaluation independently, and inter-rater reliability was computed. In instances of discord, a consensus was attained following collaborative examination.

Epidural scar adhesions scoring

Epidural scar adhesion was graded using a grading system devised by He et al. [8] Grade 0 indicates, no scar tissue on the dura mater; Grade 1 indicates, a thin fibrous band between dura mater and scar tissue; Grade 2 indicates, scar tissue in less than two-thirds of the laminectomy defect; and Grade 3 indicates, scar tissue covering more than two-thirds of the laminectomy defect or extending to the nerve roots. Subsequently, the dura mater thickness was measured (at three different points) using a magnification of 400X. In addition, the presence of arachnoid involvement was also recorded.

Scaring density scoring

Scaring density was also assessed based on the myofibroblast differentiation and categorized to: grad 0: differentiated myofibroblast less than 10%, grade 2: differentiated myofibroblast 11–50%, Grade 3: differentiated myofibroblast 51–75%, and grade 4: differentiated myofibroblast greater than 76%.

Inflammation scoring

Finally, inflammation was graded into 0 = absent inflammation, 1 = mild cellular infiltrates of neutrophils which may be mixed with few lymphocytes with mild tissue edema, 2 = moderate mixed cellular infiltrate with tissue edema may be noticed and 3 = severe cellular infiltrate with marked edema and altered normal tissue pattern.

The mRNA measurements of IL-6 and TGF-β1

According to Heid et al. [34], the mRNA levels of IL-6 and TGF-β1 were assessed 30 days postoperatively. Five rats were euthanized in a humane manner, and the scar tissues from the sites where the laminectomy was performed were collected. Total RNA extraction was done utilizing Trizol reagent, and the RNA (2 µg) was transcribed into cDNA utilizing a Promega reverse transcriptase kit. The qRT-PCR, a triple quantitative technique, was conducted using the Bio-Rad MYIQ2 (USA) instrument, following the methodology described in a previous study. The primer sequences for the investigated genes are provided in (Table 1). The amplification of GAPDH was utilized as an internal control.

Statistical analysis

The results were analyzed utilizing the 22nd version of SPSS software (IBM, USA). Verification of data normality was performed using the Shapiro test. Quantitative results were expressed using means ± SE. A one-way ANOVA test followed by Tukey's post-hoc test was employed to compare various groups. The Chi square test (Pearson and Exact Fisher) was utilized to determine the significance of the association between the different groups and as well as the qualitative data (epidural scar adhesion scores). P-value < 0.05 was considered statistically significant. Cohen's kappa statistics were utilized to evaluate the inter-observer agreement in order to guarantee that all of the evaluators were consistent with one another.

Results

Characterization of Chi/Ag-NPs

The UV–vis spectroscopic measurement was used to investigate the in situ electrochemical synthesis of Ag-NPs within the electrolyte of a Chi solution due to the distinctive observation of surface plasmon resonance.

Table 1 Showing the primer sequences for the studied genes (IL-6 and TGF-β1)

Gene	Sequence	Product size
GAPDH	Forward: CTCTGCTCCTCCCTGTTCTA Reverse: AGTTGAGGTCAATGAAGGGG	187
IL-6	Forward: GAAGTTAGAGTCACAGAAGGAGTG Reverse: GTTTGCCGAGTAGACCTCATAG	105
TGF-β1	Forward: TGCTAATGGTGGACCGCAA Reverse: CACTGCTTCCCGAATGCTGA	101

The (Fig. 2A) demonstrates the presence of a maximum at 420 nm, which can be attributed to the surface plasmon resonance of AgNPs. This observation aligns with findings from prior research indicating the presence of spherical nanoparticles which is also confirmed later by TEM results. Additionally, an absorption peak has been observed at a wavelength of 250 nm, indicating the potential formation of a [chitosan]-Ag + complex [35]. The zeta potential of AgNPs within the polymer matrix CS was measured yielding a value of + 27.9 ± 9.35 mV [36]. The positive surface charge of the AgNPs arises from the increased abundance of protonated NH3 + groups present in the solution (Fig. 2B). The generation of favorable electrostatic repulsion among the particles can lead to enhanced stability [37].

The formation of spherical AgNPs within the Chi matrix is depicted in (Fig. 2C) after a two-hour electrosynthesis process. SAED pattern as represented in (Fig. 2C), which exhibits a combination of observed ring patterns and diffraction spots. Therefore, it indicates that the AgNPs formed possess a polycrystalline structure [33]. The determination of the size distribution of the AgNPs, as depicted in (Fig. 2D), demonstrated a highly homogeneous distribution of AgNPs with a narrow average size of 4.2 nm. The small size of silver particles can be ascribed effective capping agent properties, which effectively envelop the nano-silver particles, thereby impeding their aggregation [28].

Finally, ICP analysis was performed in order to quantify the concentration of silver (Ag). Dat revealed that the concentration of silver detected in CS-AgNPs is 1196 mg/L, which is deemed to be an acceptable quantity of silver that has been released electrochemically within the polymeric matrix.

Macroscopic assessment of epidural scar adhesion

The grades of epidural scar adhesion in rats were evaluated according to Rydell's classification as shown in Fig. 3. The grades of epidural scar adhesion in rats were statically evaluated. Data showed a significant association (Pearson $X^2 = 54.071$, df = 12, *P*-value = < 0.0001) between different interferences and the Rydell's score. The laminectomy group significantly exhibited a grade 3 score (90%, *P*-value = < 0.0001). PRF was non-significantly different (fisher's exact = 5.900, df = 4, *P*-value = 0.197) from Chi/Ag-NPs in reduction of the score grade. Interestingly, the

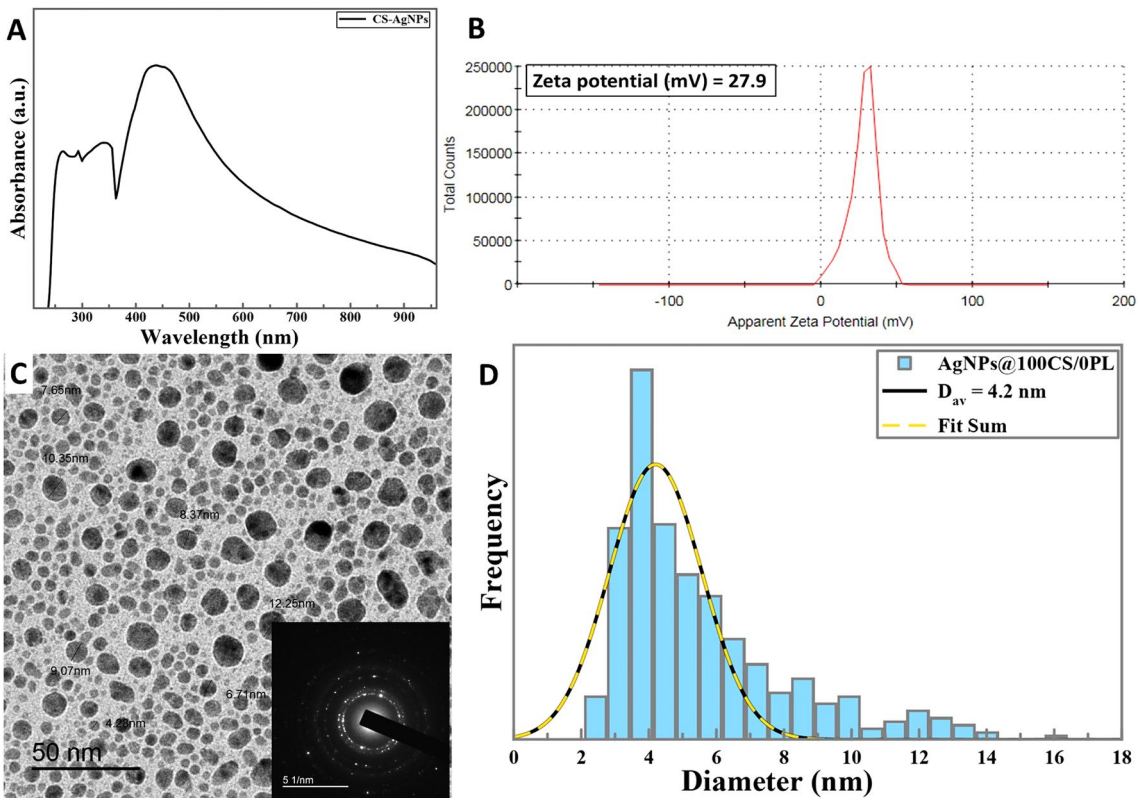

Fig. 2 Represents the characteristic properties of the prepared system **a** UV–vis spectra of CS-AgNPs sample, **b** Zeta potential distribution of the prepared CS-AgNPs sample, **c** TEM image for the prepared CS-AgNPs sample with inset of the SAED patterns, and **d** the size distribution of the formed AgNPs

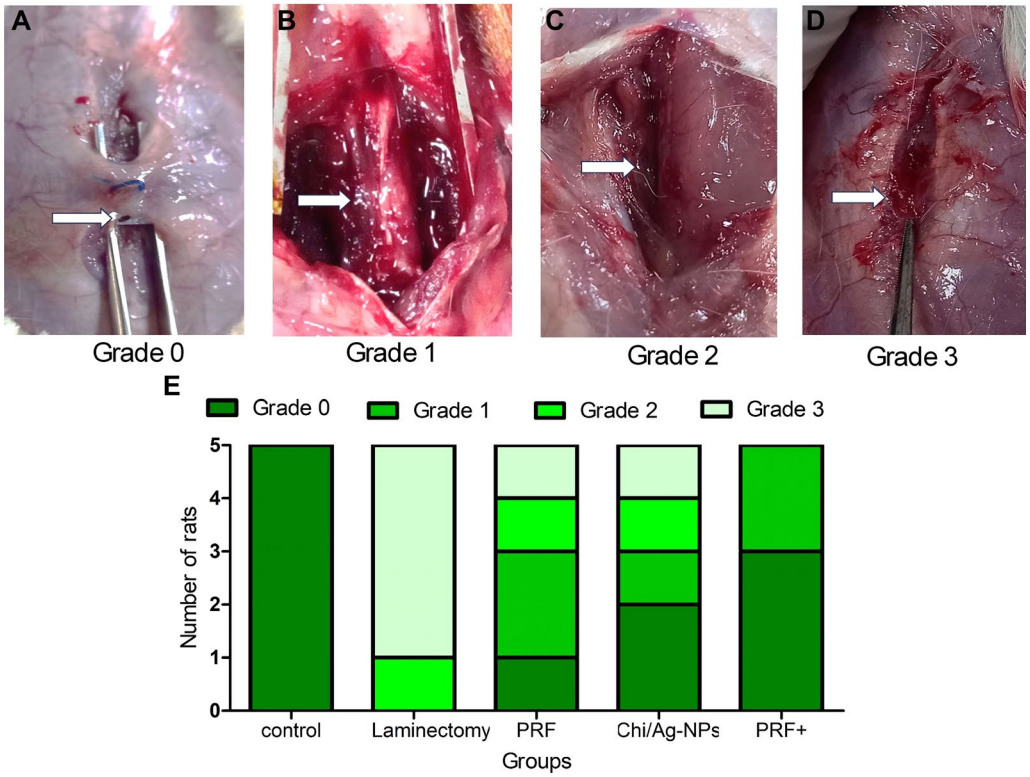

Fig. 3 Represents Macroscopic assessment of epidural scar adhesion **a** grade0 = epidural scar tissue indicates non- adherence to the dura mater in control group; **b** grade 1 = epidural scar tissue adherence to the dura mater but could be easily dissected in combined group; **c** grade 2 = epidural scar tissue adherence to the dura mater and challenging to separate without damaging the dura mater in PRF and Chi/Ag-NPs groups; **d** grade 3 = epidural scar tissue was firmly adherent to the dura mater and could not be dissected in laminectomy group. **e** showed Grades of epidural scar adhesion in rats, according to the Rydell standard. #5 rats were selected from each treatment group. (statistically analyzed by Chi square test). Combined group more significantly decrease in epidural scar adhesion compared with laminectomy group and other treated groups

PRF + Chi/Ag-NPs group showed a non- significant (fisher's exact = 3.810, df = 1, *P*-value = 0.141) difference from the control group (score grades (0 = 50% and 1 = 50%) (Fig. 3).

Histological analysis

Hematoxylin and eosin-stained control group vertebral sections showed normal spinal cord, arachnoid, dura mater, and bone structures were seen in vertebral sections from control normal group (Fig. 4A). In the laminectomy group, excessive epidural deposition of scar tissue, massive inflammation, granuloma formation and dystrophic calcification were observed around the spinal cord, leading to increased thickness of the dura mater and marked adhesion with the Pia mater. In addition, excessive deposition of scar tissue with or without adherence to dura mater, heavy leukocytic cell infiltration, granuloma formation, and dystrophic calcification were detected in vertebral sections from the laminectomy group (Fig. 4B–D). PRF group sections showed moderate inflammation and epidural scar tissue formation (Fig. 4E). While milder inflammation and more epidural scar tissue formation were detected in the Chi/Ag-NPs group, leading to focal adhesion of Pia to dura mater (Fig. 4F). Interestingly, a very mild Epidural scar fibrosis was seen in a combined treated group (Fig. 4G). Other images of the different groups are available as supplementary data files.

Masson-stained sections showed no fibrous tissue in control group (Fig. 5A), while excessive fibrosis was shown in the laminectomy group sections with granuloma formation around the spinal cord and increased dura mater thickness that penetrates nervous tissue in some sections (Fig. 5B, C). Treated groups sections showed markedly decreased epidural fibrous tissue formation in the PRF group (Fig. 5D). Denser epidural scar tissue formation was detected in the Chi/Ag-NPs group (Fig. 5E). While mild epidural scar adhesion was found in the combined treated group (Fig. 5F). Microscopic pictures showed markedly increased dura mater thickness in the Laminectomy group section, which was mitigated in the treated groups to variable levels (Fig. 6). Other

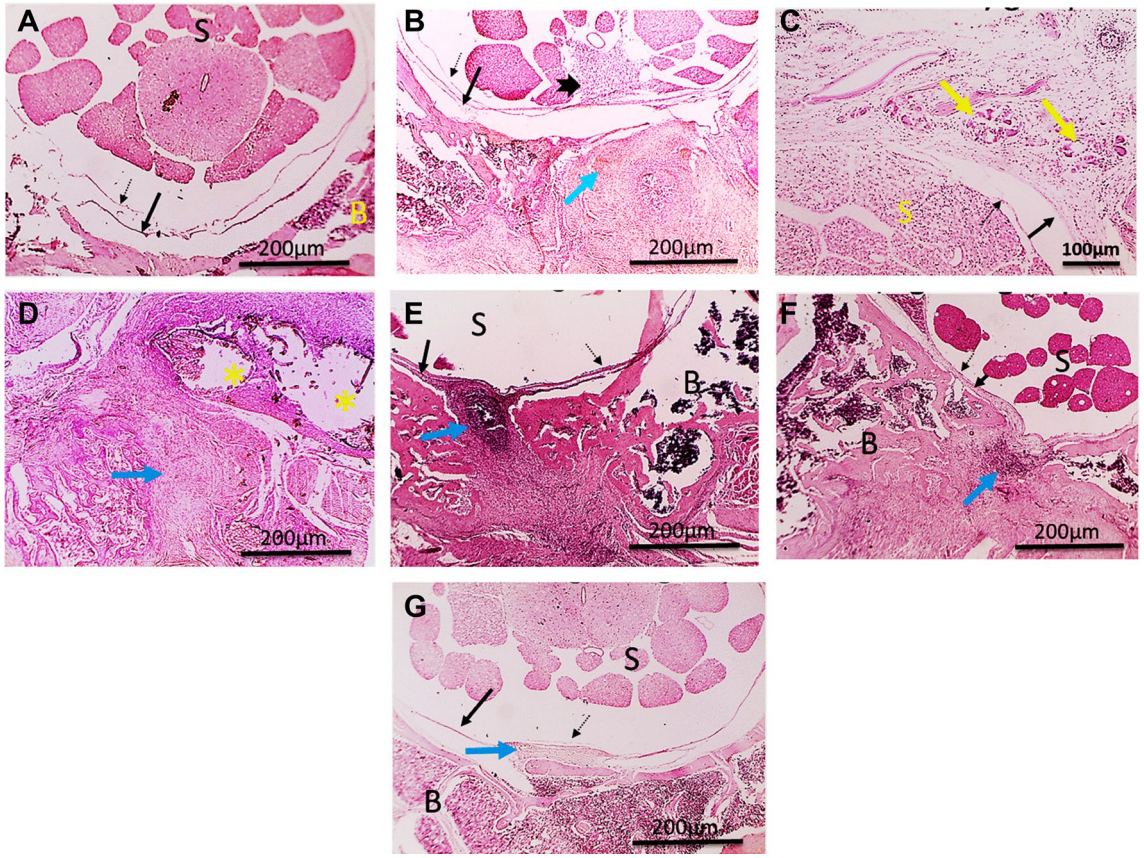

Fig. 4 Microscopic pictures showing normal structures of Pia mater (dashed black arrow); Dura mater (black arrow); B: Bone; S: spinal cord in control normal group (**A**). Excessive epidural deposition of scar tissue (blue arrow), massive Inflammation (thick black arrow), granuloma formation (yellow arrow) and dystrophic calcification (*) are seen around spinal cord leading to increased thickness of dura mater and marked adhesion with Pia mater in laminectomy group (grade 3 epidural fibrosis) (**B–D**). Moderate inflammation and epidural scar tissue formation (blue arrow) are seen in group PRF group (**E**). Milder inflammation and more epidural scar tissue formation (blue arrow) is seen in Chi/Ag-NPs group leading to focal adhesion of Pia to Dura mater (**F**). Very mild epidural fibrosis (blue arrow) is seen in group combined treatments group (**G**). Pia mater (dashed black arrow); Dura mater (black arrow); B: Bone; S: spinal cord H&E, X: 40 bar 200 µm

images of the different groups are available as supplementary data files.

Histological grading of epidural scar adhesion

According to He at el. [8], grades of epidural scar adhesion were statically shown in (Fig. 7A). The results showed a significant difference between the different groups. The laminectomy group (P-value ≤ 0.0001) exhibited epidural scar adhesion scores 2 (40%) and 3 (60%). However, the Chi/Ag-NPs group was non-significant (P-value $= 0.227$) in epidural scar adhesion reduction from the laminectomy group. In contrast, PRF and PRF + Chi/Ag-NPs groups showed significant (P-value $= 0.003$) reduction in epidural scar adhesion compared to laminectomy group but still significant from control group. Both PRF and PRF + Chi/Ag-NPs groups were non-significant from each other ($P \leq 0.650$), Also arachnoid involvement according to Cemil et al. [38] was observed with statistically significant difference between the laminectomy and the combined treatment group treated group rats (P-value $= 0.023$) (Fig. 7B**).**

The statistical analysis of scar tissue density scores revealed a significant decrease in both the treated PRF and the combined groups compared to laminectomy groups (Fig. 7C). Statistical analysis revealed a significant reduction in dura mater thickness across all treated groups compared to the laminectomy group (Fig. 7D).

Expression of TGF-β1 coding genes, fibrosis marker, was markedly elevated (P-value < 0.0001) in the laminectomy group compared to controls. Treated groups showed significantly (P-value < 0.0001) lower expression than the laminectomy group. Interestingly the combined treatment group showed significantly lower levels of the studied gene expression than each treatment alone (Fig. 7E).

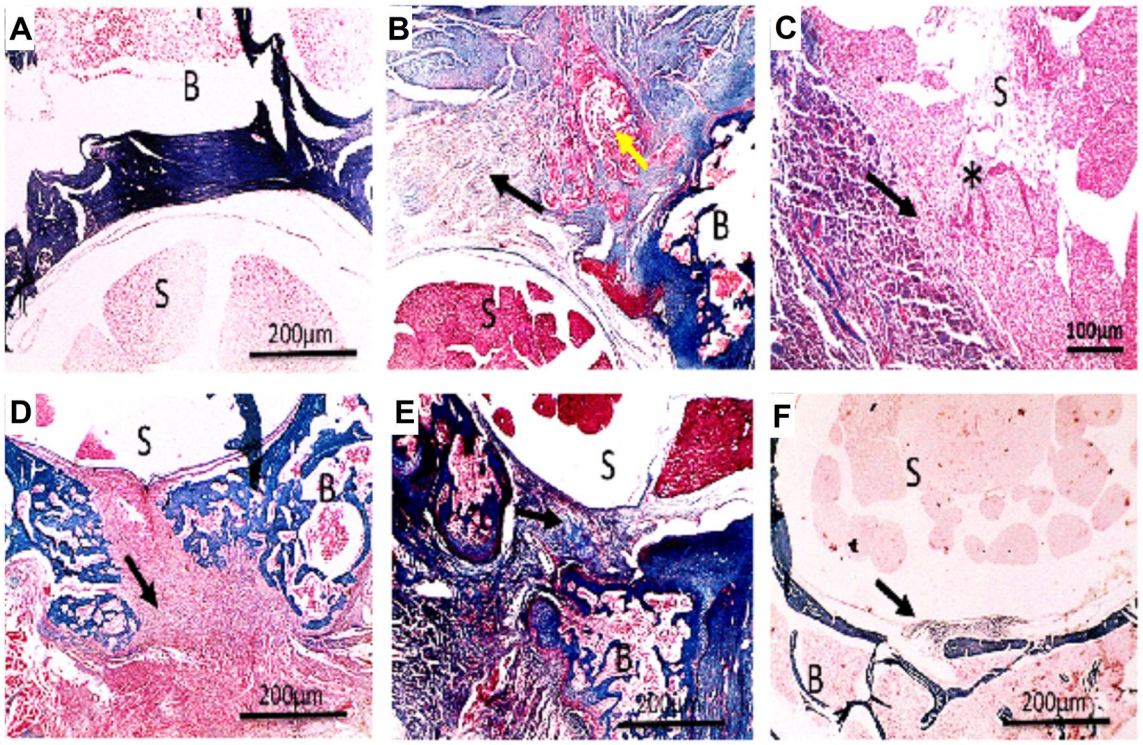

Fig. 5 Microscopic pictures showing no fibrous tissue deposition in control group (**A**). Excessive epidural deposition of fibrous tissue is seen in laminectomy group (black arrow) with granuloma formation (yellow arrow) around spinal cord accompanied by increased thickness of dura mater that invade nervous tissue (*) in some sections (**B**, **C**). Markedly decreased epidural fibrous tissue formation (black arrow) is seen in PRF group (**D**). Denser epidural scar tissue formation (black arrow) is seen in Chi/Ag-NPs group (**E**). Very mild epidural fibrosis (black arrow) is seen in the combined PRF and Chi/Ag-NPs treatment group (**F**). B: Bone; S: spinal cord. MT, X: 40 bar 200 µm

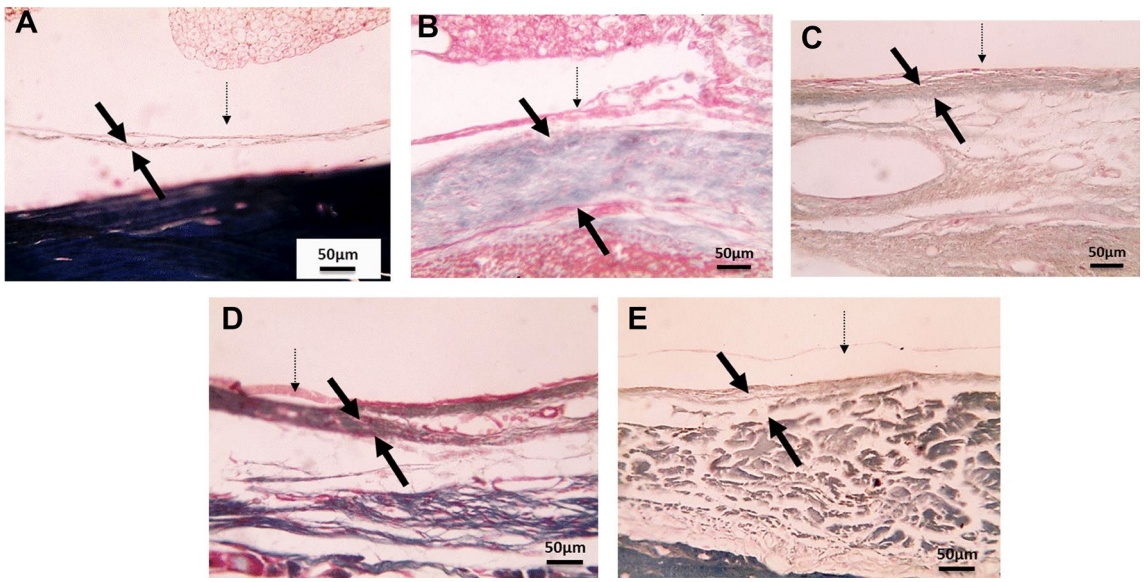

Fig. 6 Microscopic pictures showing decreased dura mater thickness in the control group (**A**), Laminectomy group (**B**), PRF treated group (**C**), Chi/Ag-NPs group (**D**), and combined PRF and Chi/Ag-NPs treatment group (**E**). MT, X: 400 bar 50 µm Pia mater (dashed black arrow); Dura mater (thin black arrow)

Inflammation scores

The inflammatory scores showed a significant decrease in Chi/Ag-NPs and combined treatment groups compared to the laminectomy group score grading (Fig. 7F). The outcomes of mRNA expression levels of IL-6 showed that IL-6 level in laminectomy group was significantly increased (6.26 ± 0.781) compared to the control group (1.032 ± 0.36). In the PRF group, the IL-6 expression level was substantially declined (*P*-value < 0.0078) compared with the laminectomy group. Conversely, its level was substantially downregulated in the Chi/Ag-NPs group compared to the laminectomy group (*P*-value < 0.0005). The IL-6 expression level in combined group significantly decreased (*P*-value < 0.0001) compared to laminectomy group and other treated groups (Fig. 7G).

Discussion

To the best of our knowledge, there was no data regarding the effect of Chi/Ag-NPs on the reduction of post laminectomy epidural scar adhesion and its combination with PRF either experimentally or clinically. Epidural scar adhesion has been identified as a major contributing factor to FBSS in patients undergoing laminectomy procedures for conditions such as disc herniation and stenosis. Due to radix compression or dural entrapment, epidural scar adhesion may lead to radicular symptoms resembling those induced by surgery; this significantly lowers the success rate of repeated surgery to a range of 5–30% [39] and worsen symptoms and pain [40]. Additionally, repeated surgeries elevate epidural scar adhesion rates, inducing persistent patient distress, consequently, epidural scar adhesion reduction is mandatory post-laminectomy, so this study aimed to eliminate epidural scar adhesion in a rat model utilizing Chi/Ag-NPs and PRF combinations.

The key mechanism in the development of EF is the rapid proliferation of fibroblasts triggered by the activation of cytokines and growth factors. This proliferation is aimed at repairing the local defective vertebral region where laminectomy is performed [41]. Epidural scar adhesion arises due to the natural wound-healing process. In patients undergoing redo surgery, the incidence of complications such as epidural hematoma, nerve root damage, dura damage, and infection increases because of adhesions and scar tissues due to epidural scar adhesion in the healing area. Consequently, research on preventing the formation of epidural scar adhesion has become increasingly significant in recent years [6, 12–16, 42–44].

The current study utilized male Sprague Dawley rats because endogenous estrogen may impact EF formation following lumbar laminectomy in rats [6]. The effect of PRF and Chi/Ag-NPs were evaluated to eliminate the post laminectomy epidural scar adhesion; PRF resulted in reduction of both inflammation and the formation of epidural scar tissue surrounding the spinal cord, in comparison to the group that underwent laminectomy without treatment. The observed effects can be ascribed to angiogenesis, enhanced osteoblast proliferation, reduced bleeding in epidural space, and tissue healing facilitated by cytokines [42, 45]. Growth factor released from platelets indicated that fibrin-containing gels alleviated epidural scar adhesion with in the first two weeks post-laminectomy, that growth factor containing platelet concentrate decreased fibrotic tissue through enhancing damaged muscle tissue reperfusion [46]. Furthermore, IL-6 and TGFβ-1 were markedly eliminated in PRF-treated rats than in the laminectomy group. This was done to validate the histopathological scoring related to aforementioned advantages of PRF.

The primary outcome suggests that PRF has the ability to stimulate the regeneration of soft tissues and promote the healing of wounds. In addition, PRF is a safe, reliable, and cost-effective option for expediting wound healing and enhancing tissue repair following damage or injury [47]. This outcome demonstrates that PRF effectively reduces epidural scar adhesion with decreased arachnoid involvement to 50% in comparison to the laminectomy group, which agrees with the prior studies published data [2, 3, 42, 48].

Chitosan has been widely applied to topical dressing in wound healing due to its stypticity, antimicrobial and nontoxic, biocompatible and biodegradable properties [49–51] with inhibition of collagen production and fibroblasts growth. Hence Chitosan can protect the spinal cord from epidural scar adhesion following disc injury [52]. Ag-NPs show great potential as antimicrobial agents because of their inherent properties and outstanding thermal stability while also demonstrating

(See figure on next page.)

Fig. 7 The histopathological and quantitative PCR evaluation of the effect of laminectomy and studied treatment PRF, Chi/Ag-NPs group, and combined PRF and Chi/Ag-NPs (PRF +) on the fibrosis and inflammation of the rats' vertebral sections. The grades of epidural scar adhesion (**A**), arachnoid involvement (**B**), scaring tissue density (**C**), dural thickness (**D**), inflammation scoring (**E**), TGF-β1 and IL-6 (**F**, **G**) coding genes expression showed that laminectomy induced fibrosis and inflammation, while the applied treatment modalities significantly improved laminectomy induced inflammation and fibrosis. Significance was evaluated by One way ANOVA test with posttest Tucky's multiple comparison test. * means *P*-value < 0.05, **means *P*-value < 0.001, while *** means *P*-value < 0.0001

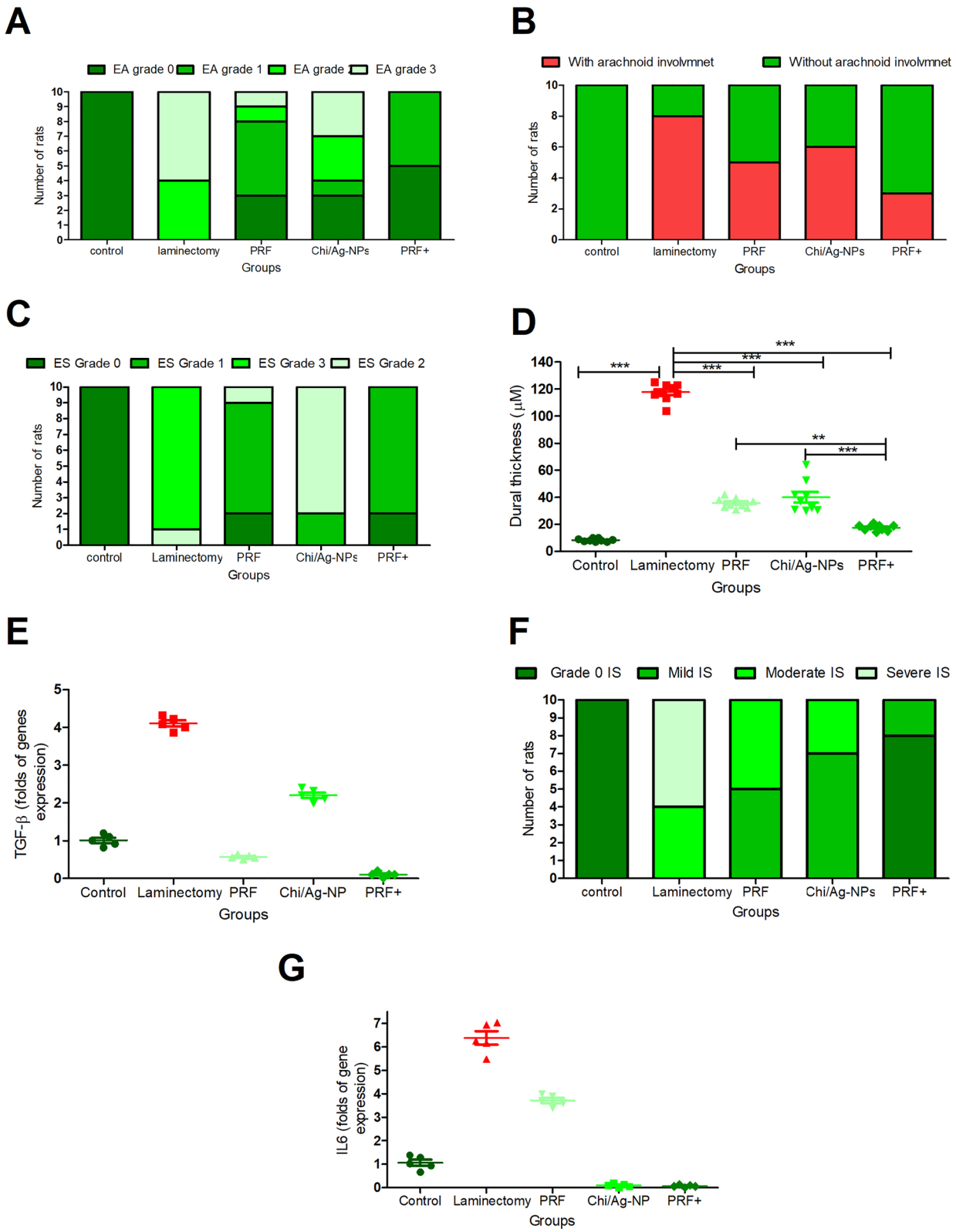

Fig. 7 (See legend on previous page.)

minimal harm to mammalian cells and tissues [53]. The utilization of silver-based antimicrobial nanocomposite materials can offer significant benefits. This can be achieved by employing a range of natural reductants, including ascorbic acid, and other biomolecular reducing agents [54, 55]. The combination of Chi/Ag-NPs created a synergistic effect, enhancing the antimicrobial properties and promoting tissue regeneration which make them ideal dermal substitute for wound healing [52, 56].

In the present study, macroscopic assessment of epidural scare adhesion in the chitosan silver nanoparticle treated group revealed significant decrease in the post-laminectomy scaring, adhesions, dural thickness, arachnoid involvmnet, as well as inflammation in comparison with the laminectomy untreated group. This result attributed to the effect of Chi/Ag-NPs, which inhibit collagen production and regulate fibroblast migration this result is consistent with the previous studies outcomes [21, 52, 54–56]. Also, IL-6 and TGFβ-1 coding genes expressions were found to significantly decreased in Chi/Ag-NPs treated rats compared to the laminectomy group. It may be attributed to TGFβ-1 and IL-6 being involved in promoting both fibroblast proliferation and collagen synthesis, as illustrated by [57].

The PRF and Chi/Ag-NPs group exhibits the presence of growth factors, including PDGF, VEGF, and TGFβ-1, which stimulate angiogenesis and enhance vascular density in the wound region [58–60]. The addition of Chi/Ag-NPs to PRF enhances its physical and chemical properties, reduces microbial activity, and is not harmful to cells. This leads to faster wound healing within 14 days. Furthermore, it demonstrates outstanding wound healing activity, and could be regarded as an effective topical burn wound healing treatment [61]. Incorporating PRF into the prepared hydrogel has an advantage in supplying growth factors, platelets, circulatory fibrocytes, and cytokines, further enhancing the wound-healing mechanism in diabetic rats [62].

In the present study, macroscopic and microscopic assessment of the rats revealed that of epidural scare adhesion in Chi/Ag-NPs combined with PRF treated group revealed that the combined effect of PRF and Chi/Ag-NPs significantly improved all studied outcome parameters regarding scaring and inflammation in comparison to each modality alone. These results may be due to the combined effect of PRF and Chi/Ag-NPs to decrease bleeding in epidural space, improve tissue healing, have an anti-inflammatory effect, regulating fibroblast migration and macrophage activation. This combination has the best effect on inflammation reduction than all treated group [58, 62].

Conclusion

Based on the findings of the study, it was found that the application of PRF with Chi/Ag-NPs on the dura after laminectomy resulted in a significant reduction in epidural scar adhesion formation after 30 days in male Spraque Dawley rats with marked decrease in the associated inflammatory response, scaring and arachnoid involvement. This conclusion was drawn based on the results of macroscopic examination, histological analysis, and mRNA expression of IL-6 and TGFβ-1.

Limitation of the study

Additional research could be beneficial in utilizing long-term duration measurement to assess the complete reduction of post-laminectomy epidural scar adhesion.

Studies on a wide range of patients may be required to understand the effect of combination groups on the reduction of epidural scar adhesion.

Supplementary Information

The online version contains supplementary material available at https://doi.org/10.1186/s12868-025-00929-9.

Additional file 1.

Additional file 2.

Additional file 3.

Additional file 4.

Additional file 5.

Acknowledgements

The authors would like to thank the staff members at MERC for their assistance and encouragement during practical work. Also great thanks to the staff members of the Department of Surgery, Anesthesiology, and Radiology, Mansoura University for their Assistance.

Author contributions

Conceived and designed the experiments: SF, AR, EM, EE. Performed the experiments: SF, MMN, WA. Analyzed the data: ASE, AZ. Wrote the paper: SF, AR, EE. All authors read and approved the manuscript.

Funding

The deanship of Scientific Research at Northern Border University, Arar, KSA, funded this research work through the project number "NBU-FFR-2025–2510-04".

Data availability

Data are available with a reasonable request to the corresponding authors.

Declarations

Ethics approval and consent to participate

The study design was approved by the Local Ethical Committee, Faculty of Veterinary medicine, Mansoura University (registration number; Ph.D./102). Ethical guidelines of the Ethics committee of national research Center-Egypt for research animal handling were applied. Animals were obtained from MERC after the ethical approval and all experiments were conducted in MERC after their approval of the study design.

Consent for publication
Not applicable.

Competing interests
The authors declare no competing interests.

Author details
[1]Medical Experimental Research Center (MERC), Faculty of Medicine, Mansoura University, Mansoura 35516, Egypt. [2]Department of Surgery, Anesthesiology and Radiology, Faculty of Veterinary Medicine, Mansoura University, Mansoura 35516, Egypt. [3]Department of Neurosurgery, Faculty of Medicine, Mansoura University, Mansoura 35516, Egypt. [4]Department of Pathology, Faculty of Veterinary Medicine, Mansoura University, Mansoura 35516, Egypt. [5]Physics Department, Faculty of Science, Mansoura University, Mansoura 35516, Egypt. [6]Physics Department, Faculty of Science, New Mansoura University, New Mansoura, Egypt. [7]Center for Health Research, Northern Border University, Arar, Saudi Arabia.

Received: 15 December 2024 Accepted: 17 January 2025
Published online: 05 February 2025

References

1. Weinstein JN, Lurie JD, Tosteson TD, Hanscom B, Tosteson AN, Blood EA, Birkmeyer NJ, Hilibrand AS, Herkowitz H, Cammisa FP, et al. Surgical versus nonsurgical treatment for lumbar degenerative spondylolisthesis. N Engl J Med. 2007;356(22):2257–70.
2. Wu CY, Huang YH, Lee JS, Tai TW, Wu PT, Jou IM. Efficacy of topical cross-linked hyaluronic acid hydrogel in preventing post laminectomy/laminotomy fibrosis in a rat model. J Orthop Res. 2016;34(2):299–306.
3. Turkoglu E, Dinc C, Tuncer C, Oktay M, Serbes G, Sekerci ZJ. Use of decorin to prevent epidural fibrosis in a post-laminectomy rat model. Eur J Pharmacol. 2014;724:86–91.
4. Karatay M, Erdem Y, Koktekir E, Erkoc YS, Caydere M, Bayar MA. The effect of bevacizumab on spinal epidural fibrosis in a postlaminectomy rat model. Turk Neurosurg. 2012;22(6):753–7.
5. Tanriverdi O, Yilmaz I, Adilay HU, Gunaldi O, Erdogan U, Gungor A, Kilic M, Tanik C. Effect of cetuximab on the development of epidural fibrosis based on CD105 and osteopontin immunohistochemical staining. Spine. 2019;44(3):E134–43.
6. Circi E, Atici Y, Baris A, Senel A, Leblebici C, Tekin SB, Ozturkmen Y. Is tranexamic acid an effective prevention in the formation of epidural fibrosis? Histological evaluation in the rats. J Korean Neurosurg Soc. 2023;66(5):503–10.
7. Erdogan B, Is M, Aker FV, Emon ST, Engin T, Akar EA, Sayman E, Somay H. Preventative effect of diclofenac sodium and/or diltiazem in rats with epidural fibrosis. Bratisl Med J. 2019. https://doi.org/10.4149/BLL_2019_135.
8. He Y, Revel M, Loty B. A quantitative model of post-laminectomy scar formation: effects of a nonsteroidal anti-inflammatory drug. Spine. 1995;20(5):557–63.
9. Kasimcan MO, Bakar B, Aktaş S, Alhan A, Yilmaz M. Effectiveness of the biophysical barriers on the peridural fibrosis of a postlaminectomy rat model: an experimental research. Injury. 2011;42(8):778–81.
10. Xu D, Zhuang Q, Li Z, Ren Z, Chen X, Li S. A randomized controlled trial on the effects of collagen sponge and topical tranexamic acid in posterior spinal fusion surgeries. J Orthop Surg Res. 2017;12(1):166.
11. Zhang C, Kong X, Liu C, Liang Z, Zhao H, Tong W, Ning G, Shen W, Yao L, Feng S. ERK2 small interfering RNAs prevent epidural fibrosis via the efficient inhibition of collagen expression and inflammation in laminectomy rats. Biochem Biophys Res Commun. 2014;444(3):395–400.
12. Song Z, Wu T, Sun J, Wang H, Hua F, Nicolas YSM, Kc R, Chen K, Jin Z, Liu JJ, et al. Metformin attenuates post-epidural fibrosis by inhibiting the TGF-β1/Smad3 and HMGB1/TLR4 signaling pathways. J Cell Mol Med. 2021;25(7):3272–83.
13. Keskin E, Tönge Ç, Kaya M, Işık E. Evaluation of the effects of berberine in the prevention of epidural fibrosis in rats: an experimental research. Saudi Med J. 2022;43(4):370.
14. Liu Y, Wang R, Han H, Li L. Tubastatin A suppresses the proliferation of fibroblasts in epidural fibrosis through phosphatidylinositol-3-kinase/protein kinase B/mammalian target of rapamycin (PI3K/AKT/mTOR) signalling pathway. J Pharmacy Pharmacol. 2022;74(3):426–34.
15. Liu P, Zhang D, Huang G, Xue M, Fang Y, Lu L, Zhang J, Xie M, Ye Z. Laminin α1 as a target for the treatment of epidural fibrosis by regulating fibrotic mechanisms. Int J Mol Med. 2023;51(1):1–11.
16. Dayanir H, Dayanir D, Emmez G, Emmez H, Akyol SN, Iseri N, Uludag OM, Kavutcu M, Ozogul C, Babacan AC. Medical ozone treatment on prevention of epidural fibrosis in the rat model. Niger J Clin Pract. 2023;26(8):1197–203.
17. Lin CY, Liu TY, Chen MH, Sun JS, Chen MH. An injectable extracellular matrix for the reconstruction of epidural fat and the prevention of epidural fibrosis. J Biomed Mater Res. 2016;11(3): 035010.
18. Agnihotri SA, Mallikarjuna NN, Aminabhavi TM. Recent advances on chitosan-based micro- and nanoparticles in drug delivery. J Control Release. 2004;100(1):5–28.
19. Mauricio Sandoval M, Claudia Albornoz R, Sonia Muñoz R, Mirta Fica R, Garcia-Huidobro I, Renato Mertens M, Ariel Hasson M. Addition of chitosan may improve the treatment efficacy of triple bandage and compression in the treatment of venous leg ulcers. J Drugs Dermatol. 2011;1(1):75.
20. Li C, Wang H, Liu H, Yin J, Cui L, Chen Z. The prevention effect of poly (L-glutamic acid)/chitosan on spinal epidural fibrosis and peridural adhesion in the post-laminectomy rabbit model. Eur Spine J. 2014;23(11):2423–31.
21. You C, Han C, Wang X, Zheng Y, Li Q, Hu X, Sun H. The progress of silver nanoparticles in the antibacterial mechanism, clinical application and cytotoxicity. Mol Biol Rep. 2012;39(9):9193–201.
22. Fong J, Wood F. Nanocrystalline silver dressings in wound management: a review. Int J Nanomedicine. 2006;1(4):441–9.
23. Liu X, Lee PY, Ho CM, Lui VC, Chen Y, Che CM, Tam PK, Wong KK. Silver nanoparticles mediate differential responses in keratinocytes and fibroblasts during skin wound healing. ChemMedChem. 2010;5(3):468–75.
24. Wong KK, Cheung SO, Huang L, Niu J, Tao C, Ho CM, Che CM, Tam PK. Further evidence of the anti-inflammatory effects of silver nanoparticles. ChemMedChem. 2009;4(7):1129–35.
25. Yadollahi M, Farhoudian S, Namazi H. One-pot synthesis of antibacterial chitosan/silver bio-nanocomposite hydrogel beads as drug delivery systems. Int J Biol Macromol. 2015;1(79):37–43.
26. Saravanan S, Nethala S, Pattnaik S, Tripathi A, Moorthi A, Selvamurugan N. Preparation, characterization and antimicrobial activity of a bio-composite scaffold containing chitosan/nano-hydroxyapatite/nano-silver for bone tissue engineering. Int J Biol Macromol. 2011;49(2):188–93.
27. Abdelgawad AM, Hudson SM, Rojas OJ. Antimicrobial wound dressing nanofiber mats from multicomponent (chitosan/silver-NPs/polyvinyl alcohol) systems. Carbohyd Polym. 2014;100:166–78.
28. Reicha FM, Sarhan A, Abdel-Hamid MI, El-Sherbiny IM. Preparation of silver nanoparticles in the presence of chitosan by electrochemical method. Carbohydr Polym. 2012;89(1):236–44.
29. Dohan DM, Choukroun J, Diss A, Dohan SL, Dohan AJ, Mouhyi J, Gogly B. Platelet-rich fibrin (PRF): a second-generation platelet concentrate. Part I: technological concepts and evolution. Oral Surg Oral Med Oral Pathol Oral Radiol Endodontol. 2006;101(3):e37-44.
30. Sun P, Miao B, Xin H, Zhao J, Xia G, Xu P, Hu J, Li Z, Li J. The effect of resveratrol on surgery-induced epidural fibrosis in laminectomy rats. Evid Based Complement Alternat Med. 2014;2014(1):574236.
31. Sangeetha R, Uma K, Chandavarkar V. Comparison of routine decalcification methods with microwave decalcification of bone and teeth. J Oral Maxillofac Pathol. 2013;17(3):386–91.
32. Bancroft JD, Gamble M. Theory and practice of histological techniques: Elsevier health sciences. 2008.
33. El-Waseif AA, Roshdy TY, Abdel-Monem MO, Hassan MG. Taguchi design analysis for optimization of probiotics cholesterol assimilation. Mater Today Proc. 2022;1(61):1154–7.
34. Heid CA, Stevens J, Livak KJ, Williams PM. Real time quantitative PCR. Genome Res. 1996;6(10):986–94.
35. Rhazi M, Desbrieres J, Tolaimate A, Rinaudo M, Vottero P, Alagui A. Contribution to the study of the complexation of copper by chitosan and oligomers. Polymer. 2002;43(4):1267–76.
36. Coseri S, Spatareanu A, Sacarescu L, Rimbu C, Suteu D, Spirk S, Harabagiu V. Green synthesis of the silver nanoparticles mediated by pullulan and 6-carboxypullulan. Carbohyd Polym. 2015;13(116):9–17.

37. Mi FL, Wu SJ, Zhong WQ, Huang CY. Preparation of a silver nanoparticle-based dual-functional sensor using a complexation–reduction method. Phys Chem Chem Phys. 2015;17(33):21243–53.
38. Cemil B, Tun K, Kaptanoglu E, Kaymaz F, Cevirgen B, Comert A, Tekdemir I. Use of pimecrolimus to prevent epidural fibrosis in a postlaminectomy rat model. J Neurosurg Spine. 2009;11(6):758–63.
39. Eldin MM, Razek NM. Epidural fibrosis after lumbar disc surgery: prevention and outcome evaluation. Asian Spine J. 2015;9(3):370.
40. Gyorfi M, Pillai I, Abdlsayed A. Spinal cord stimulation efficacy and erroneous conclusions of the cochrane library review of spinal cord stimulation for low back pain by Traeger et al. Brain Sci. 2023;13(8):1181.
41. Lv P, Zhao J, Su W, Liang X, Zhang K. An experimental novel study: hyperbaric oxygen treatment on reduction of epidural fibrosis via down-regulation of collagen deposition, IL-6, and TGF-β1. Eur J Orthop Surg Traumatol. 2015;25(Suppl 1):S53-58.
42. Demirel E, Yildiz K, Çadirci K, Aygün H, Şenocak E, Gündoğdu B. Effect of platelet-rich fibrin on epidural fibrosis and comparison to ADCON® Gel and hyaluronic acid. Acta Orthop Traumatol Turc. 2018;52(6):469–74.
43. Ismailoglu O, Kizilay Z, Cetin NK, Topcu A, Berber O. Effect of Curcumin on the formation of epidural fibrosis in an experimental laminectomy model in rats. Turk Neurosurg. 2019;29(3):440–4.
44. Yilmaz A, Karatay M, Yildirim T, Celik H, Sertbas I, Erdem Y, Caydere M, Isik HS, Bayar MA. Prevention of epidural fibrosis using Ranibizumab in a postlaminectomy rat model. Turk Neurosurg. 2017;27(1):119–23.
45. Todeschi J, Dannhoff G, Coca AH, Timbolschi DI, Proust F, Lefebvre F, Lelievre V, Poisbeau P, Vallat L, Salvat E. Effect of an intraoperative periradicular application of platelet-rich fibrin (PRF) on residual post-surgical neuropathic pain after disc herniation surgery: study protocol for Neuro-PRF, a randomized controlled trial. Trials. 2023;24(1):1–10.
46. Anitua E, Pelacho B, Prado R, Aguirre JJ, Sánchez M, Padilla S, Aranguren XL, Abizanda G, Collantes M, Hernandez M, et al. Infiltration of plasma rich in growth factors enhances in vivo angiogenesis and improves reperfusion and tissue remodeling after severe hind limb ischemia. J Control Release. 2015;202:31–9.
47. Ding Y, Cui L, Zhao Q, Zhang W, Sun H, Zheng L. Platelet-rich fibrin accelerates skin wound healing in diabetic mice. Ann Plast Surg. 2017;79(3):e15–9.
48. Miron RJ, Fujioka-Kobayashi M, Bishara M, Zhang Y, Hernandez M, Choukroun J. Platelet-rich fibrin and soft tissue wound healing: a systematic review. Tissue Eng Part B Rev. 2017;23(1):83–99.
49. Kojima K, Okamoto Y, Kojima K, Miyatake K, Fujise H, Shigemasa Y, Minami S. Effects of chitin and chitosan on collagen synthesis in wound healing. J Vet Med Sci. 2004;66(12):1595–8.
50. Rabea EI, Badawy ME, Stevens CV, Smagghe G, Steurbaut W. Chitosan as antimicrobial agent: applications and mode of action. J Biol Macromol. 2003;4(6):1457–65.
51. Xia CS, Hong GX, Dou RR, Yang XY. Effects of chitosan on cell proliferation and collagen production of tendon sheath fibroblasts, epitenon tenocytes, and endotenon tenocytes. Chin J Traumatol. 2005;8(6):369–74.
52. Marcol W, Wlaszczuk P, Palen P, Larysz-Brysz M. Prevention of epidural fibrosis by a chitosan and/or alginate gel in a rat laminectomy model. Acta Neurobiol Exp. 2013;(73).
53. Chen X, Schluesener HJ. Nanosilver: a nanoproduct in medical application. Toxicol Lett. 2008;176(1):1–12.
54. Moritz M, Geszke-Moritz M. The newest achievements in synthesis, immobilization and practical applications of antibacterial nanoparticles. J Chem Eng. 2013;228:596–613.
55. Wang LS, Wang CY, Yang CH, Hsieh CL, Chen SY, Shen CY, Wang JJ, Huang KS. Synthesis and anti-fungal effect of silver nanoparticles–chitosan composite particles. Int J Nanomed. 2015;1:2685–96.
56. You C, Li Q, Wang X, Wu P, Ho JK, Jin R, Zhang L, Shao H, Han C. Silver nanoparticle loaded collagen/chitosan scaffolds promote wound healing via regulating fibroblast migration and macrophage activation. Sci Rep. 2017;7(1):10489.
57. Katzel EB, Wolenski M, Loiselle AE, Basile P, Flick LM, Langstein HN, Hilton MJ, Awad HA, Hammert WC, O'Keefe RJ. Impact of Smad3 loss of function on scarring and adhesion formation during tendon healing. J Orthop Res. 2011;29(5):684–93.
58. Mirjalili F, Mahmoodi M. Controlled release of protein from gelatin/chitosan hydrogel containing platelet-rich fibrin encapsulated in chitosan nanoparticles for accelerated wound healing in an animal model. Int J Biol Macromol. 2023;225:588–604.
59. Qian B, Yang Q, Wang M, Huang S, Jiang C, Shi H, Long Q, Zhou M, Zhao Q, Ye X. Encapsulation of lyophilized platelet-rich fibrin in alginate-hyaluronic acid hydrogel as a novel vascularized substitution for myocardial infarction. Bioact Mater. 2022;7:401–11.
60. Rahman MM, Garcia N, Loh YS, Marks DC, Banakh I, Jagadeesan P, Cameron NR, Yung-Chih C, Costa M, Peter K. A platelet-derived hydrogel improves neovascularisation in full thickness wounds. Acta Biomater. 2021;136:199–209.
61. Borhani M, Dadpour S, Haghighizadeh A, Etemad L, Soheili V, Memar B, Vafaee F, Rajabi O. Crosslinked hydrogel loaded with chitosan-supported iron oxide and silver nanoparticles as burn wound dressing. Pharm Dev Technol. 2023;28(10):962–77.
62. Choudhary M, Chhabra P, Tyagi A, Singh H. Scar free healing of full thickness diabetic wounds: a unique combination of silver nanoparticles as antimicrobial agent, calcium alginate nanoparticles as hemostatic agent, fresh blood as nutrient/growth factor supplier and chitosan as base matrix. Int J Biol Macromol. 2021;178:41–52.

Publisher's Note